Austin Journal of Medical Oncology

Open Access

Austin Publishing Group

Research Article

The Novel Small Molecule Inhibitor, OSU-T315, Suppresses Vestibular Schwannoma and Meningioma Growth by Inhibiting PDK2 Function in the AKT Pathway Activation

Mercado-Pimentel ME[1,2,3], Igarashi S[1,2], Dunn AM[1,2], Behbahani M[1,2], Miller C[1,2], Read CM[1] and Jacob A[1,2,3,4]*

[1]Ear Institute, University of Arizona, USA
[2]Department of Otolaryngology, University of Arizona, USA
[3]Arizona Cancer Center, University of Arizona, USA
[4]BIO5 Institute, University of Arizona, USA

***Corresponding author:** Jacob A, Department of Otolaryngology, University of Arizona, Tucson, USA

Received: April 05, 2016; **Accepted:** April 18, 2016; **Published:** April 21, 2016

Abstract

Activation of PKB/AKT signaling, which requires PDK1 and PDK2 function, drives Vestibular Schwannoma (VS) and meningioma growth. PDK2 function is defined as a molecule that phosphorylates AKT-Ser473. Integrin-Linked Kinase (ILK) functions as PDK2 in PKB/AKT activation in many cancers; therefore, we hypothesized that OSU-T315, a small molecule ILK inhibitor, will inhibit the ILK-PDK2 function in PKB/AKT signaling activation in VS and meningioma cell growth. OSU-T315 decreased cell viability at IC50 < 2μM in VS (HEI193) and meningioma (Ben-Men-1) cell lines, in primary cells at < 3.5μM, while in normal primary Schwann cells at 7.1μM. OSU-T315 inhibits AKT signaling by decreasing phosphorylation at AKT-Ser473, AKT-Thr308, ILK-Ser246 and ILK-Thr173. In addition, OSU-T315 affected the phosphorylation or expression levels of AKT downstream proliferation effectors as well as autophagy markers. Flow cytometry shows that OSU-T315 increased the percentage of cells arrested at G2/M for both, HEI193 (39.99%) and Ben-Men-1 (26.96%) cells, compared to controls (21.54%, 8.47%). Two hours of OSU-T315 treatment increased cell death in both cell lines (34.3%, 9.1%) versus untreated (12.1%, 8.1%). Though longer exposure increased cell death in Ben-Men-1, TUNEL assays showed that OSU-T315 does not induce apoptosis. OSU-T315 was primarily cytotoxic for HEI193 and Ben-Men-1 inducing a dysregulated autophagy. Our studies suggest that OSU-T315 has translational potential as a chemotherapeutic agent against VS and meningioma.

Keywords: PDK2; Integrin-linked kinase; AKT; OSU-T315; Vestibular schwannoma; Autophagy

Abbreviations

NF2: Neurofibromatosis Type 2; VS: Vestibular Schwannoma; PKB/AKT: Protein Kinase B/v-Akt Murine Thymoma Viral Oncogene Homolog; PI-3K: Phosphatidylinositol 3 Kinase; PIP2: Phosphatidylinositol diphosphate; PIP3: Phosphatidylinositol Triphosphate; Thr: Threonine; Ser: Serine; PDK: Phosphoinositide-Dependent Kinase; mTORC2: Mammalian Target of Rapamycin Complex 2; ILK: Integrin-Linked Kinase; PAK1: P21-Activated Kinase 1; LC3: Light Chain 3; Atg: Autophagy-Related; GSK-3β: Glycogen Synthase Kinase -3 beta; OSU-T315: Ohio State University-T315; IC50: Inhibitory Concentration at 50%; PI: Propidium Iodide; si RNA: Small Interference Ribonucleic Acid

Introduction

Neurofibromatosis type 2 (NF2) is an autosomal-dominant familial syndrome caused by a loss-of-function mutation in the NF2 gene, which is localized on chromosome 22 and encodes the tumor suppressor protein, merlin. NF2 syndrome occurs in 1:25,000 individuals. Presenting around 20 years of age, NF2 primarily affects the nervous system, eyes and skin [1]. Abnormalities in the nervous system include bilateral vestibular schwannomas (VS) and meningiomas, among others. VS are benign intracranial tumors that originate along the vestibulocochlear nerve and cause hearing loss, tinnitus and imbalance [2]. Present treatment options are limited to surgery or radiation. Unfortunately, the former poses a number of serious risks, including cerebrospinal fluid leaks, meningitis, intracranial hemorrhage, stroke, coma and death, while the latter raises concerns of near-term treatment failure, latent tumor growth, malignant transformation, and secondary skull-base malignancies [3,4]. There is currently no FDA approved chemotherapeutic agents to treat NF2-associated tumors due to a poor understanding of the molecular mechanisms involved in this disease. However, recent studies have revealed key molecules that play a role in the growth and development of vestibular schwannoma tumors.

The serine/threonine kinase Protein Kinase B (PKB)/AKT, modulates several downstream molecules involved in cell survival, growth and proliferation. We have previously shown that the PI-3K (Phosphatidylinositol 3 Kinase)/AKT signaling is activated in VS [5]. Activation of the PI-3K/AKT pathway requires PI-3K to catalyze the phosphorylation reaction of Phosphatidylinositol Diphosphate (PIP2) to Phosphatidylinositol Triphosphate (PIP3), which recruits AKT to the lipid raft compartments in the cell membrane. This

Jacob et al. © All rights are reserved

Citation: Mercado-Pimentel ME, Igarashi S, Dunn AM, Behbahani M and Miller C, et al. The Novel Small Molecule Inhibitor, OSU-T315, Suppresses Vestibular Schwannoma and Meningioma Growth by Inhibiting PDK2 Function in the AKT Pathway Activation. Austin J Med Oncol. 2016; 3(1): 1025.

event facilitates the subsequent phosphorylation of AKT-Thr308 and AKT-Ser473 by Phosphoinositide-Dependent Kinase (PDK)1 and PDK2, respectively [6]. Both AKT-Thr308 and AKT-Ser473 phosphorylation are highly induced by upstream signals [7,8]. PDK1 is a well-described single molecule in all cells; however, studies on AKT-Ser473 phosphorylation have implicated the Rictor-Mtor Complex (mTORC2), Integrin-Linked Kinase (ILK) and rictor/ILK complex, among other kinases, to act as a "PDK2" [9-14].

ILK interacts with the cytoplasmic beta1 subunit of integrins, to regulate adhesion-mediated migration, invasion, proliferation, anchorage independent growth, and survival [9]. Deregulation of ILK has been implicated in the pathogenesis of several human malignancies, including ovarian carcinoma, melanoma, and glioblastomas, among others [15]. Together, these studies indicate that ILK has autonomous function and is also an important upstream kinase for activation of AKT, thereby regulating cell processes required for cell survival, such as suppressing apoptosis and promoting cell cycle progression.

ILK is a 59 KDa cytoplasmic serine-threonine protein kinase made up of four ankyrin repeats at the N-terminus that facilitate protein interaction, a central pleckstrin homology-like domain (pH) that mediates phosphoinositide binding, and a C-terminal kinase domain, which acts to phosphorylate downstream targets such as AKT (at Ser473). Supporting this idea, studies using COS-1 and NIH 3T3 cells show that PAK serves as a scaffold to activate PDK1 and aid in the recruitment of AKT to the membrane [16]. Additional biochemical, co-immunoprecipitation, and mutation analyses show that the binding region of PIP3 in ILK is important for AKT phosphorylation [13]. These studies show that ILK complexes with AKT and PDK1, and that ILK can disrupt the PDK1/AKT association allowing phosphorylated ILK-Ser343 in the activation loop to phosphorylate AKT at Ser473.

A more relevant study in breast cancer cell lines has shown that P21-Activated Kinase 1 (PAK1) activates ILK by phosphorylating threonine-173 and serine-246, aiding in cell proliferation and motility [17]. Additional studies by Kissil et al. have shown that over expression of the NF2 protein, merlin, inhibits PAK activation, while the loss of merlin increases it [18]. This PAK activation may in turn be causing high activation of the ILK-signaling pathway in NF2 deficient tumors.

Though the role of autophagy in cancer progression is controversial, several studies have shown that autophagy and apoptosis mutually and negatively regulate each other [19-21]. While autophagy impacts the turnover of protein aggregates and damaged organelles, apoptosis eliminates unwanted cells entirely. Both processes appear to interlink in determining the fate of a given cell. Caspases are the main initiators of apoptosis and potentially mediate the complex crosstalk between autophagy and apoptosis. Caspase-9 is involved in processing apoptotic downstream effector caspases such as caspase-3, -6 and -7. Caspase-9 has also been shown to regulate autophagy-mediated cell survival in breast cancer cells [22]. Though several studies show molecules involved in the participation of caspase-9 in autophagy or apoptosis, [23] more work is needed to reveal the molecular mechanisms whereby caspase-9 participates in regulating the two processes. The autophagic marker, LC3 (light chain 3) is a homologue of the yeast Atg8 and it is found in humans in three isoforms, LC3 A, LC3 B and LC3 C. LC3 undergoes post-translational modification to yield LC3-I, which is lipidated by the Atg5-Atg12 conjugate to become associated as LC3-II with authophagic vesicles [24-26].

In recent years, ILK and AKT inhibition have been suggested as exciting targets for drug development against human cancers and vestibular schwannomas [27,28]. OSU-T315 has been reported as a novel ILK inhibitor that induces autophagy and apoptosis in prostate and breast cancer cell lines [29]. Here, we report initial validation studies of OSU-T315 as a potential treatment for vestibular schwannomas and meningiomas. Exposure of HEI193 schwannoma and Ben-Men-1 meningioma cells to OSU-T315 caused a significant decrease in cell viability at low micro-molar IC50 (inhibitory concentration 50%) concentrations, and this effect was correlated with the AKT pathway inhibition, cell cycle arrest at G2/M, and cell death by deregulated autophagy. We report that OSU-T315 is an inhibitor of the cell survival PKB/AKT pathway via deactivation of PAK and ILK in schwannoma and meningioma cells, indicating that it is a promising new agent for preclinical drug development against NF2-associated tumors.

Materials and Methods

Cells

Cell lines: HEI193 and Ben-Men-1 cell lines are immortalized human vestibular schwannoma and benign meningioma cells respectively. HEI193 cells have a mutation in the NF2 gene causing a splicing defect in the NF2 transcript but expressing moderately the active growth suppressive, merlin [30]. Ben-Men-1 cells lack one copy of chromosome 22 and the other allele has a mutation in exon 7, which causes a premature stop codon and therefore do not express merlin [31].

Primary cells: Cells were retrieved from tumors of sporadic vestibular schwannoma and meningioma patients. Institutional Review Board protocols for the acquisition of surgically removed VS specimens are in place. VS and meningioma cells were identified with S100 and Epithelial Membrane Antigen (EMA) markers, respectively, and visualized with confocal microscope. Cell lines and primary cells were tested for contamination and authenticated by immunohistochemistry.

Cell culture

Cell lines were plated at $7.5X10^3$ cells/well in 96-well plates at 37° C, 5% CO2 overnight in complete medium (DMEM high glucose supplemented with 10% FBS) for Ben-Men-1 and HEI193 (plus 100 IU/ml penicillin-streptomycin) cells. Primary cells isolated from fresh VS tumors were grown in DMEM/10% FBS, 10 ng/mL β-heregulin (R&D Systems) and 0.2μM Forskolin (sigma) under the same conditions as the cell lines.

Cell viability and cell cycle proliferation assays

MTT Assay: The treatment efficacy of OSU-T315 (OSUCCC Medicinal Chemistry Shared Resources) against HEI193, Ben-Men-1 and primary cells was measured by detecting reduction of the tetrazolium salt, MTT (3-(4,5- dimethylthiazole-2-yl)-2,5-diphenyl-tetrazolium bromide), to formazan. Cell lines and primary cells were seeded at $7.5X10^3$ and $2X10^4$ cells/well in 96-well plates respectively,

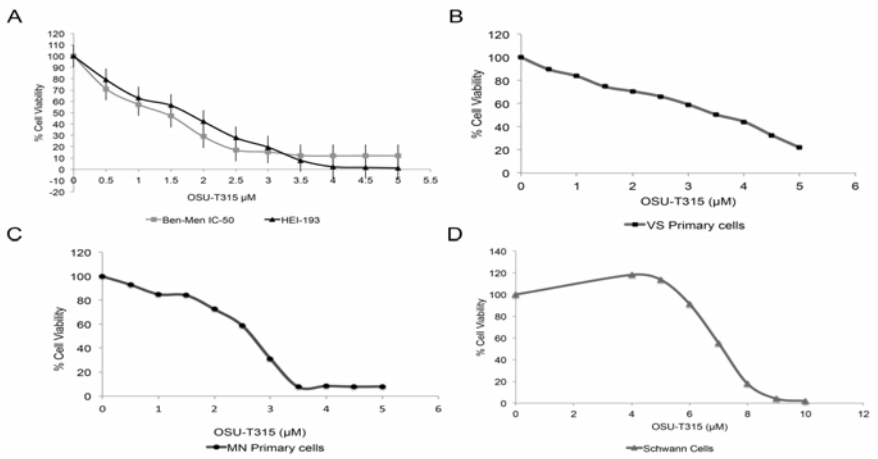

Figure 1: OSU-T315 affects cell viability in HEI193 and Ben-Men-1 cells at low micro molar concentrations.
A. OSU-T315 reduces cell viability in a dose dependent manner in HEI193 and Ben-Men-1 cells at IC50 1.82 µM and 1.58 µM respectively. **B**. OSU-T315 inhibits cell viability in primary vestibular schwannoma cells at IC50 3.41 µM. **C.** Primary meningioma cell viability was inhibited at 2.52 µM of OSU-T315. **D.** OSU-T315 decreases cell viability in normal Schwann cells at 7.1 µM. Four quantitative assays were performed to define the inhibition range in cell viability. Results from all experiments are shown as mean values, error bars show S.D.

and treated with OSU-T315 in a dose dependent manner ranging from 0.5 – 5µM (0.5, 1, 1.5, 2.0, 2.5, 3, 3.5, 4, 4.5 and 5) versus untreated controls for 72 hours at 37°C, 5% CO_2. Experiments were repeated at least four times and each drug concentration was tested in quadruples. MTT assay was performed according to Porchia et al. [32]. Briefly, cells were incubated with 200 µl of 0.5 mg/ml of MTT (Alfa Aesar, # 298-93-1) in complete medium for 4 hours, followed with 200 µl of DMSO/well and incubated for 5 min. Colorimetric readings were performed in the BioTek Synergy HT plate reader at 540 nm, and the 50% inhibitory concentration (IC50) was calculated using linear regression.

Flow Cytometry/FACS (Fluorescent Activated Cell Sorter)

Cell cycle analysis: HEI193 cells were treated with 2.5 and 5µM of OSU-T315 for 24 hours while Ben-Men-1 cells were treated with 1, 2, 3 and 4 µM of OSU-T315 for 24 hours. After incubation, floating cells were harvested and combined with trypsinized adherent cells. Cells were washed with cold PBS, pelleted at 12,000 rpm for 10 min, re-suspended in 1 ml ice-cold 70% ethanol and fixed overnight at -20°C. Fixed cells were washed with cold PBS and resuspended in 1 ml cold PBS. To ensure only DNA staining, 500µg/ml of RNase A (Sigma-Aldrich) and 40 µg/ml of Propidium Iodide (PI) (Sigma-Aldrich) were added. Cells were stained at 37° C, 5% CO2 for 30 min.

Apoptosis analysis: HEI193 and Ben-Men-1 cells were seeded at $7X10^5$ cells/100 mm culture plates. Cells were treated with 1, 2, 3, 4 µM of OSU-T315 versus non-treated cells in triplicates for 2, 24, 48 and 72 hours at 37°C, 5% CO2. Cells were trypsinized and re-suspended in 10ml of cold PBS. Pelleted cells were stained with 100µl of 1µg/ml of PI in Annexin binding buffer. Staining of the cells with Annexin V conjugates for flow cytometry analysis was carried out according to the Alexa Fluor 488 Annexin V Dead Cell Apoptosis Kit (Molecular Probes #A13201). Flow cytometry was performed using the BD FACScan and the Modfit software.

TUNEL apoptosis assay

HEI193 and Ben-Men-1 cells were seeded at $7X10^4$ cells/cover slips for 24 hours and treated with 2 and 4 µM of OSU-T315 versus untreated negative controls. Positive controls were treated with DNase I for 20 minutes. TUNEL staining was performed according to Click-iT® TUNEL Alexa Fluor® Imaging Assay (Invitrogen) instructions. Briefly, cells were fixed with 3.7% paraformaldehyde, permeabilized with 0.25% Triton-X 100 in PBS1X, and probed with the EdUTP nucleotide mixture. Fixed and stained cells were then examined using a fluorescence deconvolution light microscope. Gray scale images were captured due to improved contrast/visualization of individual cells. Images were processed and assembled using Adobe Photoshop CS6.1. Auto Contrast tool was applied to the negative control images to better visualize the cells.

Western blots

Sub-confluent cells were treated with 0, 2.5 and 5µM of OSU-T315 for 48 and 72 hours for cell lines, and 72 hours for primary cells. Cells were then harvested and homogenized in lysis buffer (1% SDS, 10mM EDTA, 50mM Tris, pH 8.1) supplemented with protease/phosphatase inhibitor cocktail (Thermo Scientific, Waltham MA). Electrophoresis was performed with 25µg or 50µg of protein/lane in a 4-20% gradient SDS- polyacrylamide gel (Thermo Scientific, Waltham MA). Proteins were transferred to PVDF membranes (Millipore, Billerica MA), and probed with specific antibodies of interest and horseradish peroxidase-conjugated secondary antibodies. The chemiluminescent signals were detected in X-ray films.

Antibodies

Antibodies were obtained from: 1) Cell Signaling Technology: Akt Antibody (#9272), Phospho-Akt (ser473) (D9E)

XP Rabbit mAb (#4060), Phospho-Akt (Thr308) Antibody (#9275), Cleaved Caspase-9 Antibody (#9509), GSK-3 β

(27C10) Rabbit mAb (#9315), Phospho-GSK-3β (Ser9) Antibody (#9336), ILK1 Antibody (#3862), LC3A (D50G8) XP Rabbit mAb (#4599) and LC3B (D11) XP Rabbit mAb (#3868). 2) Sigma-Aldrich: Monoclonal Anti- β–Actin (A1978). 3) Thermo Scientific: phospho-ILK pThr173 Antibody (PA5-12917), Phospho-ILK pSer246

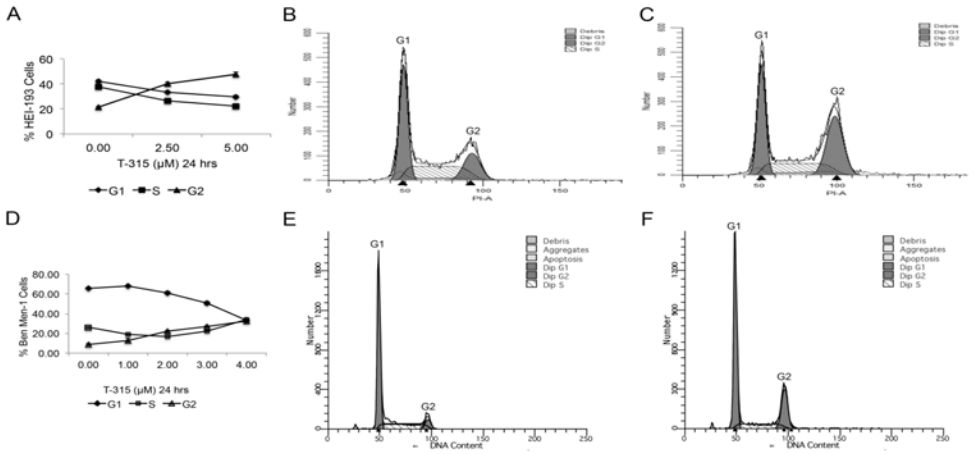

Figure 2: OSU-T315 halts cell cycle of schwannoma and meningioma cells at G2/M. A. The percentage of HEI193 cells treated with OSU-T315 significantly increases at G2/M in a dose dependent manner while the percentage of cells at G1 and S phases decreases. **B.** Representative flow cytometry graph of untreated HEI193 cells shows the majority of the cells at G1 and S phases (43.69% and 35.59% respectively), while 20.72% of the cells are at G2/M. C. Representative graph of HEI193 cells treated with 2.5 μM of OSU-T315 for 24 hours shows increased percentage of the schwannoma cells at G2/M (37.41%), and decreased percentages of the cells at G1 and S phases (35.24% and 27.35%) compared to the control (B). **D.** The percentage of Ben-Men-1 cells treated with OSU-T315 for 24 hours increases at G2/M phase, while decreasing at G1 in a dose dependent manner. E. Representative flow cytometry graph of Ben-Men-1 control cells shows a high percentage of cells at G1 phase (67.35%), while a low percentage of cells are at G2/M (7.16%); cells in S phase are at 25.49%. F. 2 μM of OSU-T315 increases the percentage of Ben-Men-1 cells at G2/M (23.54%), while the percentage of cells at G1 and S phases decreases to 60.15% and 16.31% respectively, compared to the control (E). Error bars represent SEM and p≤ 0.001.

Polyclonal Antibody (PA5-12943), Aurora-B Polyclonal Antibody (PA5-14076). Dilutions of all primary and secondary antibodies were 1:1000 and 1:10,000 respectively.

Results

OSU-T315 suppresses schwannoma and meningioma proliferation at low micromolar concentrations

OSU-T315 inhibited proliferation of vestibular schwannoma HEI193 cells, and meningioma Ben-Men-1 cells in a dose dependent manner, with IC50 values of 1.82 and 1.58 μM respectively (Figure 1A). OSU-T315 treatment of primary vestibular schwannoma and meningioma cells decreased cell viability at IC50, 3.41 μM and 2.52 μM respectively (Figure 1B and 1C), while in normal Schwann cells it decreased cell viability at 7 μM (Figure 1D). These data indicate that OSU-T315 is a putative selective drug for VS and meningioma treatment.

OSU-T315 inhibits cell cycle progression in schwannoma and meningioma cell lines

Untreated HEI193 schwannoma cell cycle was primarily in G1 (42.28%) and S phases (37.69%), while fewer cells were in G2/M phase (21.54%). In contrast, 24-hours of 2.5 μM treatment with OSU-T315 induced G2/M arrest with G1: 33.57%, S: 26.49% and G2/M: 39.99% (Figure 2A, 2B and 2C). The effect of OSU-T315 in Ben-Men-1 meningioma cells was similar, the percentage of cells at G2/M (26.96%) increased after 24-hours treatment compared to non-treated cells, 8.47% (Figure 2D, 2E and 2F). These results show that OSU-T315 inhibits the cell cycle at G2/M checkpoint in schwannoma and meningioma cells.

OSU-T315 induces cell death in vestibular schwannoma and meningioma cell lines

Biparametric cytofluorimetric analyses of Annexin V-Alexa Fluor 488 conjugates and Propidium Iodide (PI) were used to detect cell death. Annexin V has high affinity to Phosphatidylserine (PS), which in apoptotic cells translocates from the inner side of the plasma membrane to the outer side membrane layer. PI will only stain cells that have lost their cell membrane integrity. Therefore, positive staining of Annexin V with negative PI staining (Annexin V + and PI-) identifies cells in early apoptotic stages while the cell membrane has not lost its integrity. Once the cell membrane loses its integrity, PI penetrates the cells and therefore double positive stained cells (Annexin V+ and PI+) are dead cells without certainty as to the mechanism of cell death. This cell population could represent late apoptotic cells as well as necrotic cells or cell death by other mechanisms [33].

Treatment of HEI193 cells with OSU-T315 for time periods, 2, 24, 48 and 72 hours did not induce apoptosis. Representative results from 2 and 24 hours treatment with IC50 doses of OSU-T315 are shown in (Figure 3A). However, 2 hours treatment did cause significant cell death, presumably by an alternate mechanism (2 μM= 34.3%, 0 μM=12.1%). The effect of OSU-T315 in Ben-Men-1 cells was then compared to HEI193. OSU-T315's IC50 exposure decreased the percentage of apoptotic Ben-Men-1 cells (0 μM= 17.11%, 2 μM= 9.7%) at 2 hours while it increased the percentage of overall dead cells (0 μM=8.1%, 2 μM= 24.1%) when compared to the untreated cells (Figure 3A). This data indicated that OSU-T315 inhibits apoptosis occurring normally in the cells while activating another mechanism of cell death.

DNA fragmentation is a late event during apoptosis [34], which can be assessed with TUNEL assay. Our flow cytometry studies showed that after 24-hours of treatment there is a remaining double positive (Annexin V + and PI+) cell population that could represent late stage apoptotic cells. TUNEL assays were performed on HEI193 and Ben-Men-1 cells treated with 2 and 4 μM of OSU-T315 for 24 hours. These TUNEL data confirmed that OSU-T315 did not induce

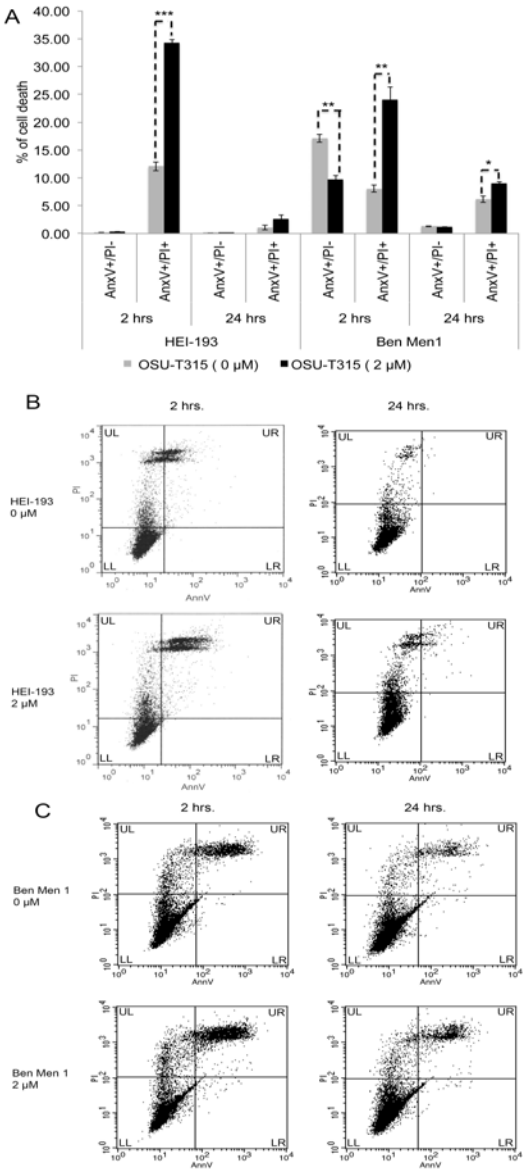

Figure 3: OSU-T315 induces cell death in HEI193 and Ben-Men-1 cells. A. Representative results from 2 and 24 hours of treatment. OSU-T315 increases significantly ($p < 0.0001$) the percentage of cell death (AnxV+/PI+) after 2 hours of treatment compared to the untreated cells. However, it does not induce apoptosis (AnxV+/PI-) in HEI193 cells through time (2 and 24 hours). In Ben-Men-1 cells, OSU-T315 decreases the percentage of apoptotic cells ($p<0.002$) while it increases cell death significantly ($p < 0.01$) after 2 hours of treatment. Ben-Men-1 cells treated for 24 hours with OSU-T315 show increased cell death with no effect in apoptosis. B. Representative flow cytometry graphs of HEI193 cells treated with OSU-T315 for 2 and 24 hours. A significant representative population of dead cells is visualized in the UR (AnxV+/PI+ cells) quadrant of the 2-hours/2 μM graph (34.8%) compared to the untreated cells (12.8%) of the 2-hours/0 μM graph. The LR quadrant does not show apoptotic (Anx+/PI-) cells at 2 and 24 hours. C. Illustrative flow cytometry graphs of Ben-Men-1 cells treated with 2 μM OSU-T315 for 2 and 24 hours *versus* untreated cells. A significant representative dense populations of dead cells are visualized in the UR quadrants of the 2 μM treatment graphs (2-hours=25.25%, 24-hours = 9.52%) compared to the 0μM graphs (2-hours = 14.54%, 24-hours = 5.55%). Cells in the upper left quadrant are Anx-/PI+, representing the possible necrotic cell population. LL quadrant contains the representative live cells (Anx-/PI-). Error bars represent SEM. $p<0.05$ = *, $p< 0.01$= ** and $p<0.001$= ***.

apoptosis in either cell line (Figure 4A and 4B) with both inhibitor concentrations. Together, these data indicated that the mechanism of cell death induced by OSU-T315 in VS and meningioma cells is not apoptosis.

OSU-T315 inhibits ILK phosphorylation and downstream PKB/AKT signaling in schwannoma and meningioma cells

ILK activity is stimulated by integrins, growth factors and chemokines, among other soluble mediators. Studies in human breast cancer cells have shown that PAK1 phosphorylates ILK at threonine-173 and serine-246 [17]. Our results showed that 2.5 and 5.0 μM of OSU-T315 decreased ILK phosphorylation at Thr-173 and Ser-246 in both HEI193 (Figure 5A and 5B) and Ben-Men-1 (Figure 5C and 5D) cells without affecting total ILK levels. To determine the effect of OSU-T315 on PKB/AKT activation, which is downstream from ILK, we assessed phosphorylation status for AKT-Ser473 and AKT-Thr308 in both cell lines with 2.5 and 5 μM of OSU-T315. HEI193 and Ben-Men-1 show a significant and progressive decrease of AKT-Ser473 and AKT-Thr308 phosphorylation while total PKB/AKT protein expression levels were stable (Figure 5E, 5F, 5G and Figure 5H).

Primary VS cells (Figure 5I) were treated with OSU-T315 at various concentrations. After 72 hours of treatment, OSU-T315 decreased ILK-Thr173 and AKT-Ser473 phosphorylation (Figure 5J and 5K). A slight increase of AKT-Thr308 is visualized in the densitometry measurements at 2.5 and 5 μM (Figure 5K). These data confirm that OSU-T315 inhibits specifically the PDK2 function in the activation of ILK-PKB/AKT signaling in primary vestibular schwannoma cells.

Our findings are consistent with our hypothesis that ILK may be functioning as a PDK2 molecule during the PKB/AKT signal activation of VS and meningioma growth. In addition, these data suggest that OSU-T315 inhibits ILK phosphorylation via PAK1 due to its decreasing effect in ILK phosphorylation at PAK1 phosphorylation sites, ILK-Ser246 and ILK-Thr173.

OSU-T315 inhibits cell proliferation and induces cell death by targeting key downstream effectors of PKB/AKT signaling molecules

Our cell cycle data show that OSU-T315 exposure arrested schwannoma and meningioma cells at G2/M. Similar studies done in glioblastomas have shown that ILK pharmacologic inhibition caused G2/M arrest, and in *Drosophila* ILK knockdown by siRNA causes abnormal mitotic spindles [35,36]. Additionally, studies in HeLa cancer cells showed that GSK (glycogen synthase kinase)-3β and AKT were localized at the centrosomes and that inhibition of GSK-3β promoted aberrations in microtubule length and chromosomal alignment during pro-metaphase [37]. To understand the effect of OSU-T315 on the cell cycle at the molecular level, we analyzed the phosphorylation and expression of GSK-3β. This molecule is constitutively active in resting cells but in stimulated cells it becomes inactivated by AKT phosphorylation on Ser-9 at the N-terminal [37,38]. Our data showed that OSU-T315 decreased GSK-3β-Ser-9 phosphorylation in HEI193, Ben-Men-1 and primary VS cells (Figure 6A, 6B, 6C and 6D), while it did not affect GSK-3β total expression levels when compared to untreated cells. These results indicated that OSU-T315 activated GSK-3β by decreasing GSK-3β-

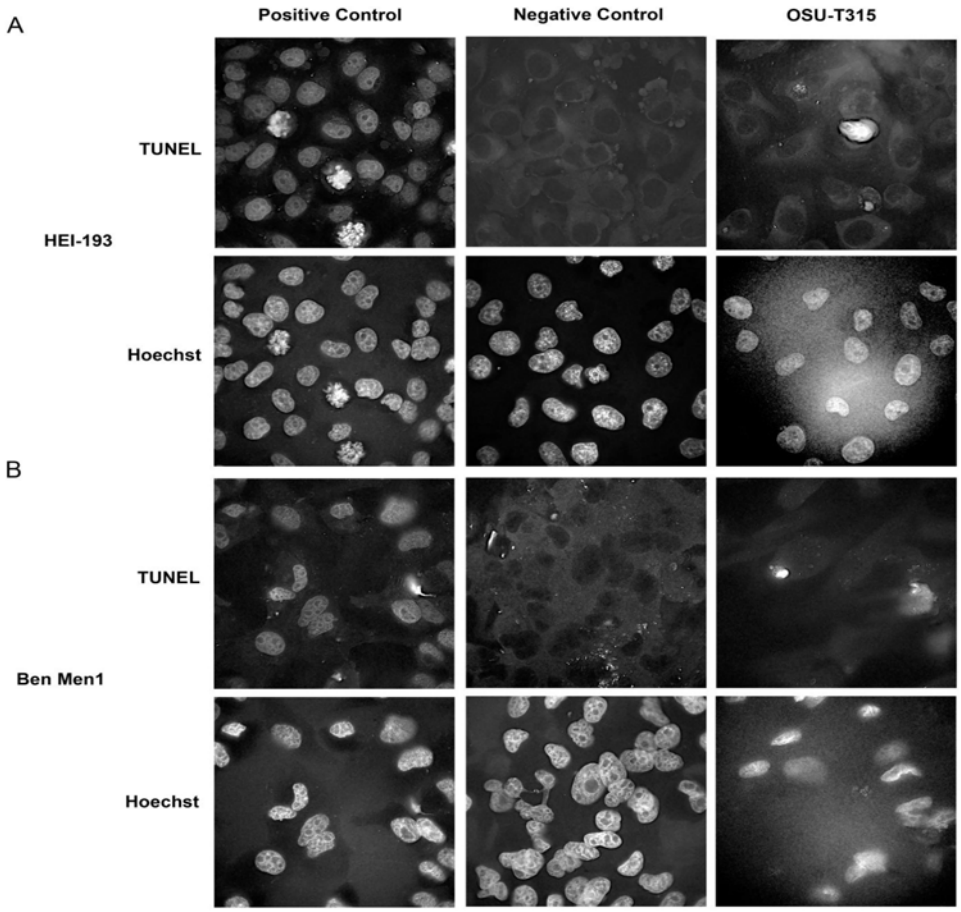

Figure 4: OSU-T315 does not induce apoptosis in HEI193 and Ben-Men-1 cells. A. Representative pictures of HEI193 cells treated with 2 μM of OSU-T315 for 24-hours do not show incorporation of EdUTP (TUNEL) compared to the positive control. Untreated cells (Negative Control) did not incorporate EdUTP. B. Representative pictures of Ben-Men-1 cells treated with 2 μM of OSU-T315 for 24-hours do not incorporate EdUTP, compared to the positive control cells treated with DNase I. Untreated OSU-T315 cells do not show EdUTP incorporation. TUNEL Assay was visualized in a deconvolution microscope under a 20X magnification.

Ser-9 phosphorylation, akin to the resting/non-proliferating state of schwannoma and meningioma cells.

Other important kinases in cell division and downstream targets of AKT are the Aurora kinases, which play crucial roles in chromosome segregation [39]. Aurora B is first detected at late G2/M phase and its inhibition causes massive polyploidization and consequently cell death [39,40]. Since ILK plays a role in mitotic spindle, we further investigated the expression level of Aurora B in HEI193 and Ben-Men-1 cells treated with OSU-T315. Forty-eight hour of OSU-T315 treatment decreased Aurora B expression levels in both cell lines (Figure 6E and 6F). Together, these data confirm that OSU-T315 exerts arrest of the cell cycle at G2/M phase of schwannoma and meningioma cells through the regulation of cell proliferation markers downstream of PKB/AKT signaling.

Several studies have shown that apoptotic and autophagic markers interlink during cell death. Since our flow cytometry data showed that OSU-T315 increased cell death of HEI193 and Ben-Men-1 cells, and our MTT assays show 50% decrease in cell viability after 72 hours of treatment, we assessed the expression levels of apoptotic and autophagic markers in 72 hours OSU-T315-treated versus non-treated cells. These data showed that increasing concentration of OSU-T315 increased caspase-9 and LC3 B expression levels in vestibular schwannoma cells while LC3 A levels decreased after 72 hours of treatment (Figure 6G, 6H and 6I). TUNEL staining, however, indicated that the increased caspase-9 activity in OSU-T315 treated cells did not induce apoptosis. In meningioma cells, caspase-9 and LC3 a levels increased with 5 μM only while LC3 B showed a marked increase at 2.5 and 5 μM. These data showed that OSU-T315 caused cell death by dysregulating the autophagy process.

Discussion

PKB/AKT is an important driver of VS and meningioma growth, and a cell-signaling pathway that positively regulates proliferation and cell survival in many cancers [5,29,41]. ILK interacts with PKB/AKT and has been suggested to function as a PDK2 molecule inducing maximal AKT activity by phosphorylation [13]. We sought to determine whether OSU-T315 inhibits PDK2 function in the activation of PBK/AKT in VS and meningioma growth, and whether this growth suppression occurs by using a putative ILK inhibitor. OSU-T315 has been reported as a novel therapeutic inhibitor that abrogates AKT activation by inhibiting AKT translocation into the lipid rafts in chronic lymphocytic leukemia cells; and an ILK inhibitor that induces autophagy and/or apoptosis in various cancer

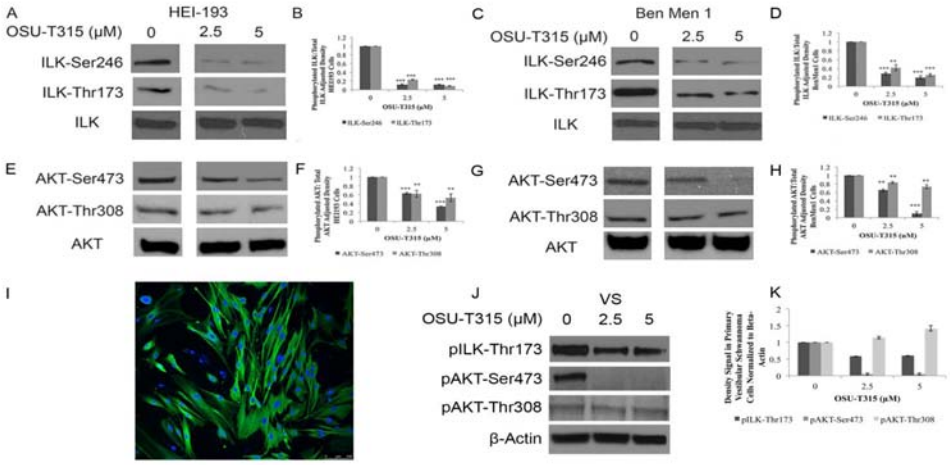

Figure 5: ILK and PKB/AKT phosphorylation is inhibited by OSU-T315 in vestibular schwannoma and meningioma cells. A. OSU-T315 decreases the phosphorylation of ILK-Ser246 and ILK-Thr173 but does not affect total ILK expression in HEI193. B. HEI193 densitometry measurements of ILK-Ser246 and ILK-Thr173 signal in western blots normalized to total ILK showing, significant decrease in phosphorylation at 2.5 and 5 μM when compared to control, 0 μM. C. OSU-T315 decreases significantly the phosphorylation of ILK-Ser246 and ILK-Thr173 but does not affect total ILK in Ben-Men-1 cells. D. Ben-Men-1 densitometry measurements of Figure C normalized to total ILK show significant decrease in phosphorylation of ILK-Ser246 and ILK-Thr173 at 2.5 and 5 μM when compared to control 0 μM. E. OSU-T315 decreases the phosphorylation of AKT-Ser473 and AKT-Thr308 but does not affect total AKT expression in HEI193. F. HEI193 densitometry measurements of AKT phosphorylation in western blots normalized to total AKT show a significant decrease in phosphorylation of AKT-Ser473 and AKT-Thr308 at 2.5 and 5 μM when compared to 0 μM. G. OSU-T315 decreases the phosphorylation of AKT-Ser473 and AKT-Thr308 but does not affect total AKT expression in Ben-Men-1 cells. H. Ben-Men-1 densitometry measurements of AKT phosphorylation normalized to total AKT (Figure G) show significant decrease in phosphorylation of AKT-Ser473 and AKT-Thr308 at 2.5 and 5 μM when compared to control, 0μM. I. Primary vestibular schwannoma cells derived from a VS patient express the S100 marker. J. OSU-T315 decreased significantly the phosphorylation levels of ILK-Thr173 and AKT-Ser473. Phosphorylation levels of AKT-Thr308 were not significantly affected. K. Densitometry measurements normalized to the loading control, β-actin, confirmed low levels of ILK and AKT phosphorylation in primary cells. Error bars represent standard deviation of three measurements of the representative western blots. $p<0.05$ = *, $p< 0.01$= ** and $p<0.001$= ***.

models [29,42]. We demonstrate here that OSU-T315 inhibits ILK phosphorylation at the ILK sites phosphorylated by PAK1, and PKB/AKT signaling in vestibular schwannoma and meningioma cells, leading to G2 cell cycle arrest and death via the deregulation of autophagy. Since activation of ILK is accomplished by PAK1 phosphorylation at ILK-Ser246 and ILK-Thr173, these studies suggest that OSU-T315 inhibits ILK by suppressing PAK1 kinase activity in VS and meningioma cells. OSU-T315 does not inhibit ILK in all cell types; for example, recent studies in chronic lymphocytic leukemia cells show that OSU-T315 inhibited the PKB/AKT pathway through mechanisms other than ILK inactivation [42]. Therefore, inhibition of ILK and PKB/AKT by OSU-T315 may be cell type specific.

Exposure of OSU-T315 halts cell cycle progression for both schwannoma and meningioma cells G2/M. G2/M phase is an important cell cycle DNA damage checkpoint that prevents the cell from entering to mitosis (M-phase) if the DNA is damaged. Aurora B expression is first localized at the G2/M phase and its inhibition causes a massive chromosome multiplication and cell death [40,43]. Correlating to these findings, our data show that OSU-T315 reduces Aurora B expression levels in HEI193 and Ben-Men-1 cells. OSU-T315 exposure activates GSK-3β (i.e. decreased GSK-3β phosphorylation), a phenomenon occurring in resting cells that fails to progress from G2 to M phase [37]. Several factors can interfere with the cell cycle progression from G2 to mitosis. Studies performed by other groups show that inhibition of GSK-3β induces defects in microtubule length and the arrangement of chromosomes during pro-metaphase [37]. Together, these immunoblot data is consistent with flow cytometry results demonstrating that schwannoma and meningioma cells fail to progress from G2 to mitosis after exposure to OSU-T315, perhaps in part through aberrations in the regrowth of the radial microtubules and damage of the DNA by polyploidization of the chromosomes. Further studies are required to confirm these important mechanisms by which this drug functions to suppress NF2-associated tumor growth at observed low micromolar concentrations.

OSU-T315 appears to be both cytostatic (cell cycle arrest) and cytotoxic in schwannoma and meningioma cells. The later mechanism of growth suppression occurs via deregulation of autophagy. Though autophagy typically allows cells to survive against prolonged starvation or any other stressful stimuli, its dysregulation is known to induce cell death. Many studies have addressed the crosstalk between apoptosis and autophagy [44]. Among the molecules involved in this crosstalk are the caspases, which play an important role in these two seemingly opposed processes. OSU-T315 treatment increases expression of caspase-9 and LC3 B while decreasing LC3 A levels in HEI193 cells. Increased caspase-9 in HEI193 cells with G2/M halted could be facilitating autophagosome formation indicated by the increased levels of LC3 B. Our data correlate with studies done by Han, et al. showing that caspase-9 facilitates autophagosome formation by interacting with Atg7 [23]. In this interacting complex, Atg7 represses caspase-9 apoptotic activity and the later enhances LC3 II formation, which is necessary for LC3 to become associated with the autophagic vesicles [23,45]. Together, these results suggest that overexpression of caspase-9 and LC3 B in OSU-T315-treated schwannoma and meningioma cells deregulate autophagy, possibly by increasing autophagosome activity. In Ben-Men-1 cells

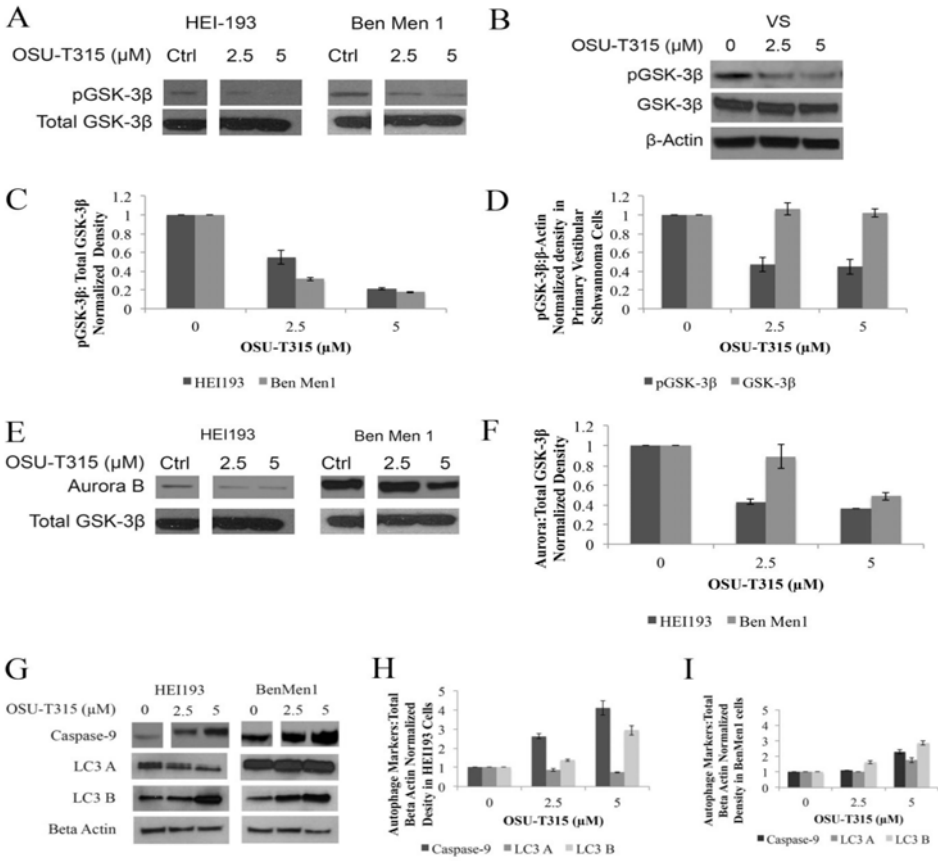

Figure 6: OSU-T315 affects downstream PKB/AKT signaling molecules involved in the growth of radial microtubules during cell proliferation and cell death by autophagy. A. Treatment of HEI193 and Ben-Men-1 with OSU-T315 decreases GSK-3β-Ser9 phosphorylation levels with 2.5 and 5 μM but not GSK-3β total expression levels. B. OSU-T315 decreased phosphorylation of GSK-3β -Ser9 in primary VS cells at 2.5 and 5 μM compared to control, 0 μM. C. Densitometry measurements normalized to total GSK-3β confirm western blot data showing decrease of GSK-3β-Ser9 phosphorylation in both cell lines, HEI193 and Ben-Men-1. D. Densitometry measurements normalized to the loading control, β-actin, confirm decrease in phosphorylation of GSK-3β-Ser9 in 18 primary VS cells. E. Expression of total aurora B decreases markedly in HEI193 with 2.5 and 5 μM of OSU T315 while in Ben-Men-1 cells decreased aurora levels are visualized with 5 μM of OSU-T315. F. Densitometry measurements of aurora B levels show a noticeable decrease at 2.5 μM in HEI193, and in Ben-Men-1cells at 5 μM compared to control, 0 μM. G. OSU-T315 treatment increases caspase-9 and LC3 B in HEI193 at 2.5 and 5μM while in Ben-Men-1 cells only LC3 B increases at the same concentrations, and caspase-9 and LC3 A increases markedly at 5 μM. H. Densitometry measurements of caspase-9, LC3 A and LC3 B confirm western blot data of HEI193 cells. I. Ben-Men-1's western blot data of G confirmed by densitometry measurements. Error bars represent standard deviation of three measurements.

OSU-T315 does not induce caspase-9 when compared to the control but it induces LC3 B expression levels, indicating the formation of autophagosomes.

Conclusion

In conclusion, our *in vitro* data reveal a mechanism of action of OSU-T315 as a drug development agent for the treatment of NF2. These data indicate that OSU-T315 behaves as a selective drug for vestibular schwannomas and meningiomas by decreasing cell viability at IC50 lower than 5 μM, while its effect in normal primary Schwann cells is at higher concentration, 7.1 μM. This new ILK/AKT inhibitor arrests the cell cycle in both type of cells, and induces cell death by dysregulating the autophagy process. These data indicate that cell cycle arrest by OSU-T315 induces cues involved in a dysregulated autophagy.

Acknowledgement

We thank Dr. Marco Giovannini and Dr. Long-Sheng Chang for graciously providing the cell lines, HEI193 and Ben- Men-1 respectively. We thank Dr. Thomas Doetschman and Renee Cercone for critical review of the manuscript. We acknowledge the technical assistance of Daniela Rolph to test the activity of the compound, OSU-T315, by MTT assay. No competing interests declared.

Funding

This work was supported by the National Institute of Deafness and Other Communication Disorders/National Institute of Health (K08 DC009644 to A. Jacob).

References

1. Evans DG, Moran A, King A, Saeed S, Gurusinghe N, Ramsden R. Incidence of vestibular schwannoma and neurofibromatosis 2 in the North West of England over a 10 - year period: higher incidence than previously thought. Otol Neurotol. 2005; 26: 93-97.

2. Welling DB, Packer MD, Chang LS. Molecular studies of vestibular schwannomas: a review. Curr Opin Otolaryngol Head Neck Surg. 2007; 15: 341-346.

3. Evans DG, Birch JM, Ramsden RT, Sharif S, Baser ME. Malignant

transformation and new primary tumours after therapeutic radiation for benign disease: substantial risks in certain tumour prone syndromes. J Med Genet. 2006; 43: 289-294.

4. Balasubramaniam A, Shannon P, Hodaie M, Laperriere N, Michaels H, Guha A. Glioblastoma multiforme after stereotactic radiotherapy for acoustic neuroma: case report and review of the literature. Neuro-oncology. 2007; 9: 447-453.

5. Jacob A, Lee TX, Neff BA, Miller S, Welling B, Chang LS. Phosphatidylinositol 3- kinase/AKT pathway activation in human vestibular schwannoma. Otology & neurotology. 2008; 29: 58-68.

6. Fresno Vara JA, Casado E, de Castro J, Cejas P, Belda-Iniesta C, González-Barón M. PI3K/Akt signalling pathway and cancer. Cancer Treat Rev. 2004; 30: 193-204.

7. Downward J. Mechanisms and consequences of activation of protein kinase B/Akt. Curr Opin Cell Biol. 1998; 10: 262-267.

8. Alessi DR, James SR, Downes CP, Holmes AB, Gaffney PR, Reese CB, et al. Characterization of a 3-phosphoinositide-dependent protein kinase which phosphorylates and activates protein kinase Balpha. Curr boil. 1997; 7: 261-269.

9. Delcommenne M, Tan C, Gray V, Rue L, Woodgett J, Dedhar S. Phosphoinositide-3-OH kinase-dependent regulation of glycogen synthase kinase 3 and protein kinase B/AKT by the integrin-linked kinase. Proc Natl Acad Sci USA. 1998; 95: 11211-11216.

10. Persad S, Attwell S, Gray V, Delcommenne M, Troussard A, Sanghera J, et al. Inhibition of integrin-linked kinase (ILK) suppresses activation of protein kinase B/Akt and induces cell cycle arrest and apoptosis of PTEN-mutant prostate cancer cells. Proc Natl Acad Sci USA. 2000; 97: 3207-3212.

11. Hresko RC, Mueckler M. mTOR.RICTOR is the Ser473 kinase for Akt/protein kinase B in 3T3-L1 adipocytes. J Biol Chem. 2005; 280: 40406-40416.

12. Sarbassov DD, Guertin DA, Ali SM, Sabatini DM. Phosphorylation and regulation of Akt/PKB by the rictor-mTOR complex. Science. 2005; 307: 1098-1101.

13. Persad S, Attwell S, Gray V, Mawji N, Deng JT, Leung D, et al. Regulation of protein kinase B/Akt-serine 473 phosphorylation by integrin-linked kinase: critical roles for kinase activity and amino acids arginine 211 and serine 343. J Biol Chem. 2001; 276: 27462-27469.

14. McDonald PC, Oloumi A, Mills J, Dobreva I, Maidan M, Gray V, et al. Rictor and integrin-linked kinase interact and regulate Akt phosphorylation and cancer cell survival. Cancer Res. 2008; 68: 1618-1624.

15. Lee SL, Chou CC, Chuang HC, Hsu EC, Chiu PC, Kulp SK, et al. Functional Role of mTORC2 versus Integrin-Linked Kinase in Mediating Ser473-Akt Phosphorylation in PTEN-Negative Prostate and Breast Cancer Cell Lines. PLoS One. 2013; 8: 67149.

16. Higuchi M, Onishi K, Kikuchi C, Gotoh Y. Scaffolding function of PAK in the PDK1-Akt pathway. Nat Cell Biol. 2008; 10: 1356-1364.

17. Acconcia F, Barnes CJ, Singh RR, Talukder AH, Kumar R. Phosphorylation-dependent regulation of nuclear localization and functions of integrin-linked kinase. Proc Natl Acad Sci USA. 2007; 104: 6782-6787.

18. Kissil JL, Wilker EW, Johnson KC, Eckman MS, Yaffe MB, Jacks T. Merlin, the product of the Nf2 tumor suppressor gene, is an inhibitor of the p21-activated kinase, Pak1. Mol Cell. 2003; 12: 841-849.

19. Gordy C, He YW. The crosstalk between autophagy and apoptosis: where does this lead? Protein Cell. 2012; 3: 17-27.

20. Mathew R, Karantza-Wadsworth V, White E. Role of autophagy in cancer. Nat Rev Cancer. 2007; 7: 961-967.

21. Nikoletopoulou V, Markaki M, Palikaras K, Tavernarakis N. Crosstalk between apoptosis, necrosis and autophagy. Biochim Biophys Acta. 2013; 1833: 3448-3459.

22. Jeong HS, Choi HY, Lee ER, Kim JH, Jeon K, Lee HJ, et al. Involvement of caspase-9 in autophagy-mediated cell survival pathway. Biochim Biophys Acta. 2011; 1813: 80-90.

23. Han J, Hou W, Goldstein LA, Stolz DB, Watkins SC, Rabinowich H. A Complex between Atg7 and Caspase-9: A Novel Mechanism of Cross-Regulation between Autophagy and Apoptosis. J Biol Chem. 2014; 289: 6485-6497.

24. He H, Dang Y, Dai F, Guo Z, Wu J, She X, et al. Post-translational modifications of three members of the human MAP1LC3 family and detection of a novel type of modification for MAP1LC3B. J Biol Chem. 2003; 278: 29278-29287.

25. Kabeya Y, Mizushima N, Ueno T, Yamamoto A, Kirisako T, Noda T, et al. LC3, a mammalian homologue of yeast Apg8p, is localized in autophagosome membranes after processing. EMBO J. 2000; 19: 5720-5728.

26. Otomo C, Metlagel Z, Takaesu G, Otomo T. Structure of the human ATG12~ATG5 conjugate required for LC3 lipidation in autophagy. Nat Struct Mol Biol. 2013; 20: 59-66.

27. Agnihotri S, Gugel I, Remke M, Bornemann A, Pantazis G, Mack SC, et al. Gene-expression profiling elucidates molecular signaling networks that can be therapeutically targeted in vestibular schwannoma. J Neurosurg. 2014; 121: 1434-1445.

28. Yau CY, Wheeler JJ, Sutton KL, Hedley DW. Inhibition of integrin-linked kinase by a selective small molecule inhibitor, QLT0254, inhibits the PI3K/PKB/mTOR, Stat3, and FKHR pathways and tumor growth, and enhances gemcitabine-induced apoptosis in human orthotopic primary pancreatic cancer xenografts. Cancer Res. 2005; 65: 1497-1504.

29. Lee SL, Hsu EC, Chou CC, Chuang HC, Bai LY, Kulp SK, et al. Identification and characterization of a novel integrin-linked kinase inhibitor. J Med Chem. 2011; 54: 6364-6374.

30. Lepont P, Stickney JT, Foster LA, Meng JJ, Hennigan RF, Ip W. Point mutation in the NF2 gene of HEI-193 human schwannoma cells results in the expression of a merlin isoform with attenuated growth suppressive activity. Mutat Res. 2008; 637: 142-151.

31. Burns SS, Akhmametyeva EM, Oblinger JL, Bush ML, Huang J, Senner V, et al. Histone deacetylase inhibitor AR-42 differentially affects cell-cycle transit in meningeal and meningioma cells, potently inhibiting NF2-deficient meningioma growth. Cancer Res. 2013; 73: 792-803.

32. Porchia LM, Guerra M, Wang YC, Zhang Y, Espinosa AV, Shinohara M, et al. 2-amino-N-{4-[5-(2-phenanthrenyl)-3-(trifluoromethyl)-1H-pyrazol-1-yl]-phenyl} acetamide (OSU-03012), a celecoxib derivative, directly targets p21-activated kinase. Mol Pharmacol. 2007; 72: 1124-1131.

33. Vermes I, Haanen C, Steffens-Nakken H, Reutelingsperger C. A novel assay for apoptosis. Flow cytometric detection of phosphatidylserine expression on early apoptotic cells using fluorescein labelled Annexin V. J Immunol Methods. 1995; 184: 39-51.

34. Collins JA, Schandi CA, Young KK, Vesely J, Willingham MC. Major DNA fragmentation is a late event in apoptosis. J Histochem Cytochem. 1997; 45: 923-934.

35. Edwards LA, Woo J, Huxham LA, Verreault M, Dragowska WH, Chiu G, et al. Suppression of VEGF secretion and changes in glioblastoma multiforme microenvironment by inhibition of integrin-linked kinase (ILK). Mol Cancer Ther. 2008; 7: 59-70.

36. Bettencourt-Dias M, Giet R, Sinka R, Mazumdar A, Lock WG, Balloux F, et al. Genome-wide survey of protein kinases required for cell cycle progression. Nature. 2004; 432: 980-987.

37. Wakefield JG, Stephens DJ, Tavaré JM. A role for glycogen synthase kinase-3 in mitotic spindle dynamics and chromosome alignment. J Cell Sci. 2003; 116: 637-646.

38. Cross DA, Alessi DR, Cohen P, Andjelkovich M, Hemmings BA. Inhibition of glycogen synthase kinase-3 by insulin mediated by protein kinase B. Nature. 1995; 378: 785-789.

39. Li JP, Yang YX, Liu QL, Zhou ZW, Pan ST, He ZX, et al. The pan-inhibitor of Aurora kinases danusertib induces apoptosis and autophagy and suppresses epithelial-to- mesenchymal transition in human breast cancer cells. Drug Des Devel Ther. 2015; 9: 1027-1062.

40. Lens SM, Voest EE, Medema RH. Shared and separate functions of polo-like kinases and aurora kinases in cancer. Nat Rev Cancer. 2010; 10: 825-841.

41. Tang X, Jang SW, Wang X, Liu Z, Bahr SM, Sun SY, et al. Akt phosphorylation regulates the tumour-suppressor merlin through ubiquitination and degradation. Nat Cell Biol. 2007; 9: 1199-1207.

42. Liu TM, Ling Y, Woyach JA, Beckwith K, Yeh YY, Hertlein E, et al. OSU-T315: a novel targeted therapeutic that antagonizes AKT membrane localization and activation of chronic lymphocytic leukemia cells. Blood. 2015; 125: 284-295.

43. Ditchfield C, Johnson VL, Tighe A, Ellston R, Haworth C, Johnson T, et al. Aurora B couples chromosome alignment with anaphase by targeting Bub R1, Mad2, and Cenp-E to kinetochores. J Cell Biol. 2003; 161: 267-280.

44. Gump JM, Thorburn A. Autophagy and apoptosis: what is the connection? Trends Cell Biol. 2011; 21: 387-392.

45. Nepal S, Kim MJ, Hong JT, Kim SH, Sohn DH, Lee SH, et al. Autophagy induction by leptin contributes to suppression of apoptosis in cancer cells and xenograft model: involvement of p53/FoxO3A axis. Oncotarget. 2015; 6: 7166-7181.

Austin J Med Oncol - Volume 3 Issue 1 - 2016
ISSN : 2471-027X | www.austinpublishinggroup.com
Jacob et al. © All rights are reserved

Citation: Mercado-Pimentel ME, Igarashi S, Dunn AM, Behbahani M and Miller C, et al. The Novel Small Molecule Inhibitor, OSU-T315, Suppresses Vestibular Schwannoma and Meningioma Growth by Inhibiting PDK2 Function in the AKT Pathway Activation. Austin J Med Oncol. 2016; 3(1): 1025.